中國機械工程學刊第四十二卷第二期第 181~186 頁(民國一百一十年)
Journal of the Chinese Society of Mechanical Engineers, Vol.42, No.2, pp 181~186 (2021)

Smooth Source-Target Maps for Freeform Lens Design for Uniform Illumination of Right Polygons

Ku-Chin Lin*****and Min-Hsiung Ma******

Keywords：freeform lens, uniform illumination, edge-ray principle.

ABSTRACT

Source-target maps play the prevailing role in freeform lens design for diverse illumination applications, but very few of previous studies have taken into account the smoothness of the map. A non-smooth map may result in a freeform lens with discontinuous surfaces or surfaces with bulge/sharp edges that will greatly increase the difficulty for lens fabrication and induce large variation in the produced irradiance distribution. In this study, a map is proposed to achieve continuous and smooth freeform surfaces for uniform illumination of right polygons. The proposed map is an integration of a number of primitive maps where a polygon is divided into a number of symmetric quadrilaterals of the same size, and the irradiance energy of source is also divided into the same number of symmetric pie sectors. The transfer of a pie sector of irradiance energy onto a quadrilateral is derived. Procedures to implement the proposed map are given in this study. The adequacy of the proposed map is demonstrated by Monte Carlo ray tracing simulation and experiment as well. The contribution of this study is fundamental and profound in the field of freeform lens design. Advanced studies for uniform illumination of arbitrary polygons are currently taken to expand the applicability of the proposed map.

INTRODUCTION

Freeform lenses have good flexibility for design to achieve diverse illumination profiles and irradiance distributions on a target plane (Ries et al., 2002; Fang et al., 2008; Chen et al., 2010; Lin, 2014). Continuous and smooth freeform surfaces are normally desired since discontinuous surfaces could greatly increase the difficulties of mold fabrication to achieve desired irradiance distributions (Luo et al., 2010; Fang et al., 2008). Slight variation of discontinuous surfaces can result in large variation in the produced irradiance distribution.

In freeform lens design, the edge-ray principle (Ries et al., 1994) is adopted. Equi-luminous fluxes of light source are usually regarded as the edge rays, and the transfer of the edge rays resembles the transfer of the irradiance energy of the source. The problem of freeform lens design is governed by a partial differential equation of the second order. The equations can be solved by a numerical method for a mesh of surface grids and spline surface construction using a CAD software (Chen et al., 2010; Lin, 2014; Luo et al., 2010). Each surface grid denotes the trace of an edge ray through the surface where the surface normals can be computed. However, there is no guarantee that a continuous and smooth surface can fit all the normals (Wu et al., 2014).

Mapping of the edge rays from a source to a target is called a source-target map (Fournier et al., 2010). The map plays the prevailing role for design of a freeform lens for accurate irradiance distributions. Smooth source-target maps are normally required to achieve smooth freeform surfaces, otherwise discontinuous surfaces or surfaces with bulge/sharp edges could be resulted.

A smooth map satisfying the so-called integrability condition for a freeform reflector can be found in (Fournier et al., 2010). The map leverages the classic property of ellipsoids where a light ray emitted from one focus is reflected to the second focus. However, the property of two foci does not fit the scope for freeform lens design. Mao *et al.* proposed an iteration method for regulating the source-target map to enhance illumination uniformity (Mao et al., 2015). Other similar methods can be found in (Wang et al., 2009; Xia et al., 2010). Among the methods, a substantial proportion is based on the

Paper Received January, 2017. Revised April, 2017. Accepted September, 2017. Author for Correspondence: Min-Hsiung Ma.

* *Professor, Department of Mechanical Engineering, Kun Shan University, Taiwan 71070, ROC.*

** *Graduate Student, Department of Mechanical Engineering, Kun Shan University, Taiwan 71070, ROC.*

source-target map, but very few of the studies have taken into account the smoothness of the map.

This study presents a smooth map for uniform illumination of right polygons. For the general purpose, a right polygon is divided into a number of symmetric quadrilaterals of the same size. Meanwhile, the irradiance energy of source is divided into the same number of symmetric pie sectors. The transfer of a pie sector of irradiance energy onto a quadrilateral is derived and it forms a primitive of the proposed map. The adequacy of the proposed map is demonstrated by Monte Carlo ray tracing simulation and experiment as well.

SYSTEM EQUATIONS AND PREVIOUS SOURCE-TARGET MAPS

Schematic of the optical system in this study is shown in Figure 1. In the system are the point source p_s at the origin of the *x*-*y*-*z* coordinate system, a freeform lens between a light source and a target plane S_d, a freeform surface of the lens denoted by S_t, and a spherical bottom surface of the lens denoted by S_b. The lens optical axis coincides with the z axis and an emitting light ray Φ intersects with S_b, S_t, and S_d at p_b, p_t and p_d, respectively.

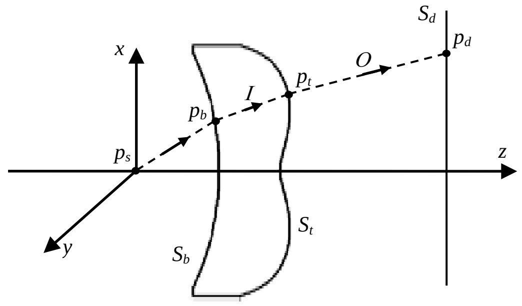

Fig. 1 Schematic of optical system.

The following partial differential equations can be developed to solve for a freeform surface mesh (Ding et al., 2008):

$$x_d - x_t = \frac{N_{tx}}{N_{tz}}[(z_d - z_t) - n\Phi_z \overline{p_t p_d}] + n\Phi_x \overline{p_t p_d}\ , \tag{1a}$$

$$y_d - y_t = \frac{N_{ty}}{N_{tz}}[(z_d - z_t) - n\Phi_z \overline{p_t p_d}] + n\Phi_y \overline{p_t p_d}\ , \tag{1b}$$

where n denotes the lens refractive index; (x_t, y_t, z_t) and (x_d, y_d, z_d) the coordinates of p_t and p_d, respectively; $[N_{tx}, N_{ty}, N_{tz}]$ the surface normal at p_t; Φ_x, Φ_y, Φ_z the *x*, *y*, and *z* components of the light ray.

At the lens bottom surface, we have

$$\rho_t \sin(\varphi_t - \varphi_s + \alpha_{bi} - \alpha_{bo}) = \overline{p_s p_b} \sin(\alpha_{bi} - \alpha_{bo})\ , \tag{2a}$$

$$\overline{p_s p_b} = \frac{R_b \sin(\varphi_s - \alpha_{bi})}{\sin \varphi_s}\ , \tag{2b}$$

where R_b the radius of the bottom surface; φ_s and φ_t denote the inclination angle of $\overline{p_s p_b}$ and $\overline{p_s p_t}$; α_{bi} and α_{bo} the incident and refractive angles of the ray.

Source-target maps are normally established based on the principle of energy conservation,

$$\sum G_S(\varphi, \theta) = \sum G_T(x, y)\ , \tag{3}$$

where $G_S(\varphi, \theta)$ denotes the grids of equi-luminous fluxes emitted from a source; it is in a spherical coordinate system where φ is the inclination angle and θ is the azimuth angle of the coordinate system; $G_T(x, y)$ denotes the grids of equi-luminous fluxes on a target plane; it is in Cartesian coordinate system.

In this study, a point source is assumed. An iso-φ profile of source is the grids of equi-luminous fluxes of the same inclination angle. An iso-φ profile of target is the grids of equi-luminous fluxes mapping on the target plane. The iso-φ contours of source are assumed concentric circles. The geometry of lens for design has a flat bottom and a freeform surface at the top of the lens.

An equation to describe many illumination profiles is given in (Mao et al., 2015),

$$\left|\frac{x}{a}\right|^n + \left|\frac{y}{b}\right|^n = 1\ , \tag{4}$$

where n is a characteristic parameter of the profiles.

Previous maps adopt a proportional ratio of the iso-φ contours to the profile, so the contours and the profile have the same shape in Figs 2 (a)-(d). For n = 2, the profile is a circle or an ellipse, and the iso-φ contours are concentric circles or ellipses. The distances between the center and the contour grids $|G_T(x, y)|$ vary smoothly with two maxima at the major axis and two minima at the minor axis as shown in Figure 2 (f). Under the proportional map, the resulting freeform surface is smooth as shown in Fig. 2(j). The irradiance distribution has good uniformity as shown in Fig. 2(n) based on 500,000 light-rays tracing simulation in LightTools. However, the proportional map becomes non-smooth as n changes.

As n = 1, the profile becomes a rhomboid. The iso-φ contours are also rhomboids in Fig. 2 (a). Singular variations of $|G_T(x, y)|$ occur at the vertices of the iso-φ contours as shown in Fig. 2(e). It results in a freeform surface with sharp edges at the diagonals of the lens as shown in Fig. 2(i), and poor uniformity of irradiance distribution is shown in Fig. 2(m).

As n = 4, the profile becomes partially flat in Fig. 2(c). The two maxima split into four. Large gradients among the contour occur as shown in Fig. 2(g). Freeform surfaces with bulges at the diagonals arise in Fig. 2(k). Large surface normal change occurs around the maxima where Fresnel loss is significant. Surfaces with bulges could greatly reduce the illumination uniformity as shown in Fig. 2(o).

As n further increases and approaches infinity, the profile becomes a rectangle, and singular variations of $|G_T(x, y)|$ occur again as shown in Figs 2(d) and 2(h). Freeform surfaces with sharp edges but worse illumination uniformity are resulted in Figs 2(l) and 2(p).

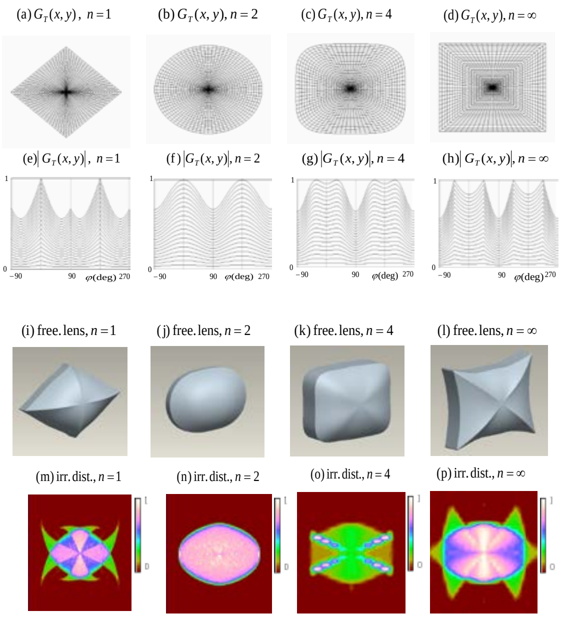

Fig. 2 $G_T(x,y)$, $|G_T(x,y)|$, freeform lenses for four different profiles, and irradiance distribution.

It is shown in the above examples that smooth source-target maps are necessary and essential conditions to achieve smooth freeform lenses without bulge/sharp surfaces. A smooth map has smooth variation and moderate gradients of the iso-φ contours. Such a map for uniform and rectangular illumination was proposed in (Lin, 2014),

$$\bar{x} = \frac{\bar{\varphi}\cos\theta}{\sqrt{1-\bar{\varphi}^2\sin^2\theta}}\ , \tag{5a}$$

$$\bar{y} = \frac{\bar{\varphi}\sin\theta}{\sqrt{1-\bar{\varphi}^2\cos^2\theta}}\ , \tag{5b}$$

where $\bar{x}$ and $\bar{y}$ denote the normalized coordinates of Cartesian system ($\bar{x} = 2x/W$, $\bar{y} = 2y/H$, W the width of the rectangle, H the height of the rectangle); $\bar{\varphi}$ the normalized inclination angle of equi-luminous flux ($\bar{\varphi} = \varphi/\varphi_{\max}$, $\varphi_{\max}$ the maximal inclination angle).

The iso-φ contours of the map are

$$\bar{\varphi} = \sqrt{\frac{\bar{x}^2+\bar{y}^2-2\bar{x}^2\bar{y}^2}{1-\bar{x}^2\bar{y}^2}} = c\ , \tag{6}$$

where c denotes a constant and $0 \le c \le 1$.

An example of the above rectangular map is given in Figure 3(a). The iso-φ contours smoothly vary from inside circle-alike contours to outside rectangle-alike ones. The variation of $|G_T(x,y)|$ is smooth as shown in Fig. 3(b). Freeform surfaces without bulge/sharp surfaces are achieved along with good illumination uniformity as shown in Fig. 3(c) and 3(d).

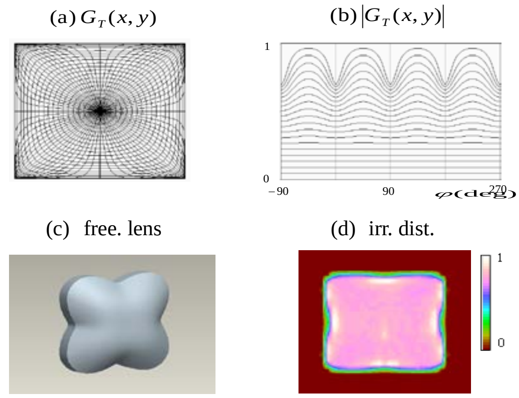

Fig. 3 $G_T(x,y)$, $|G_T(x,y)|$, freeform lenses for uniform rectangular illumination, and irradiance distribution.

PROPOSED SOURCE-TARGET MAPS FOR RIGHT POLYGONAL PROFILES

In this study, a polygon is divided into a number of symmetric quadrilaterals of the same size. Meanwhile, the irradiance energy of source is also divided into the same number of symmetric pie sectors. The transfer of a pie sector of irradiance energy onto a quadrilateral forms a primitive of the proposed map. The number of pie sectors equals the number of quadrilaterals and the edges of the polygon.

Examples of right polygons are shown in Figure 4 where a quadrilateral is one-third of the triangle, one-fourth of the rhomboid, and one-fifth of the pentagon. Since scaling and rotation do not change the smoothness of the mapping, the sizes of the polygons can be proportionally adjusted such that the irradiance circle of source in solid line is circumscribed by the polygon in dashed line.

In Fig. 4, P_0 denotes the geometric center of both the polygon and the source. P_1 and P_3 are midpoints of the polygon edges. P_2 is a polygon vertex. $P_0P_1P_3$ denotes a pie sector. $P_0P_1P_2P_3$ denotes a quadrilateral. The quadrilateral is self symmetric at $\overline{P_0P_2}$ and symmetric with its neighboring quadrilaterals at $\overline{P_0P_1}$ and $\overline{P_0P_3}$. The pie sector has similar symmetric properties. Due to the symmetry, the energy transfer from a pie sector to a quadrilateral serves as a primitive of the proposed map. For this reason, the derivation for a primitive map is only given below.

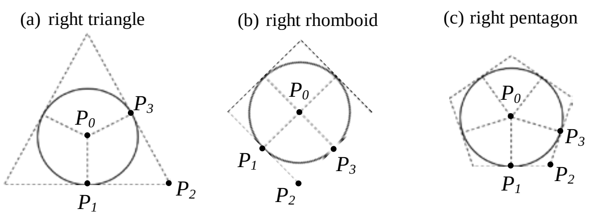

Fig. 4 Pie sectors and quadrilaterals of a right polygon.

For each of the quadrilaterals, an area-affine coordinate system is constructed as shown in Figure 5, and

$$\frac{\overline{P_0P_{03}}}{\overline{P_0P_3}}=\frac{\overline{P_1P_{12}}}{\overline{P_1P_2}}, \tag{7a}$$

$$\frac{\overline{P_0P_{01}}}{\overline{P_0P_1}}=\frac{\overline{P_3P_{32}}}{\overline{P_3P_2}}, \tag{7b}$$

$$u=\frac{Area\ \ of\ quadrilateral\ P_0P_1P_{03}P_{12}}{Area\ \ of\ quadrilateral\ P_0P_1P_2P_3}, \tag{7c}$$

$$v=\frac{Area\ \ of\ quadrilateral\ P_0P_{01}P_{32}P_3}{Area\ \ of\ quadrilateral\ P_0P_1P_2P_3}, \tag{7d}$$

where (u, v) denotes the affine system coordinate and $u, v \in [0,1]$.

In Fig. 5, points of a blue line have the same u coordinate, and of a red line have the same v coordinate. The coordinate scales are the same due to the symmetry of the quadrilaterals. If the quadrilaterals are counted in counterclockwise, the u-axis of one system overlaps with the v-axis of its next neighbor, and the v-axis overlaps with the u-axis of its previous neighbor.

In Fig. 5, S is a grid point of pie sector. Its mapping image in the quadrilateral is denoted by T. The primitive map is

$$T(x,y)=S(x,y)+\Delta S_u+\Delta S_v, \tag{8a}$$

$$\Delta S_u=S_u(x,y)-S(x,y), \tag{8b}$$

$$\Delta S_v=S_v(x,y)-S(x,y), \tag{8c}$$

$$\overline{P_{01}S_u}=\frac{\overline{P_{01}S}}{\overline{P_{01}S_u^*}}\overline{P_{01}P_{32}}, \tag{8d}$$

$$\overline{P_{03}S_v}=\frac{\overline{P_{03}S}}{\overline{P_{12}S_v^*}}\overline{P_{03}P_{12}}, \tag{8e}$$

where P_{01}, P_{03}, P_{12}, P_{32} are the edge points of the quadrilateral; S_u^*, S_v^* the intersection points between the pie sector curve and $\overline{P_{01}P_{32}}$, and $\overline{P_{03}P_{12}}$, respectively, and

$$P_{03}(x,y)=(1-u)P_0(x,y)+uP_3(x,y), \tag{9a}$$

$$P_{12}(x,y)=(1-u)P_1(x,y)+uP_2(x,y), \tag{9b}$$

$$P_{01}(x,y)=(1-v)P_0(x,y)+vP_1(x,y), \tag{9c}$$

$$P_{32}(x,y)=(1-v)P_3(x,y)+vP_2(x,y), \tag{9d}$$

The proposed map is formed by integrating all the primitive maps after proper scaling and rotation. The integration becomes Eqs (5) if the polygon is a square. However, the closed-form formula for a general right polygon are not available now. As an alternative, procedures for computation of the proposed map are given:

1. Create uniform u- and v-array for a quadrilateral in Cartesian and area-affine coordinate using Eqs (7c) and 7(d).
2. For each grid point S of the pie sector, compute the mapping image T in the quadrilateral by interpolation for the edge points P_{01}, P_{03}, P_{12}, P_{32} and the intersection points S_u^*, S_v^*, and then using Eqs (8).
3. Perform the scaling and rotation to achieve all the other primitive maps.
4. Integrate all the primitive maps to achieve the proposed source-target map.

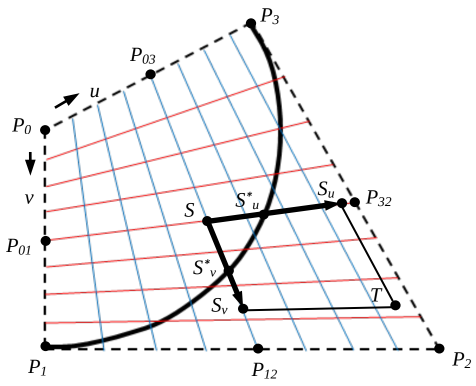

Fig. 5 Schematic of a primitive map.

The adequacy of the proposed map has been tested by simulation for several polygonal illuminations and lens sizes_with a flat bottom. The iso-φ contours of all primitive maps join smoothly between the neighboring quadrilaterals after integration. The contours vary from inside circle-alike contours to outside polygon-alike. The computations involved to solve Eqs (1) and (2) for generating the freeform surface grids are performed by LabVIEW codes written by the author. With the surface grids, the CAD software ProE is employed to construct a freefrom lens which is then imported into the software LightTools for performing ray-tracing simulations. For the polygons in Fig. 4, the proposed maps has been applied. The results for a Lambertian LED light are shown in Figure 6(a)~6(c). The variations of $|G_T(x,y)|$ are smooth as shown in Fig. 6(d)~6(f). Smooth freeform lenses are achieved as shown in Fig. 6(g)~6(i). The lens surfaces are singled out with slightly different curvatures which resemble the polygons although the shapes are distorted. Good uniformity of irradiance distribution by simulation are shown in Fig. 6(j)~6(l).

The above freeform lenses designed by the proposed map have been manufactured in PMMA by CNC machining with labor-intensive polishing applied to the lens surfaces. The labor polishing induces imprecision about 0.03mm. However, precise illumination profiles and good uniformity of irradiance distribution are achieved as shown in Figure 7 where rounded profiles at the vertices and imprecise irradiance cut at the edges are due to the manufacturing imprecision and the point source assumption made in this study.

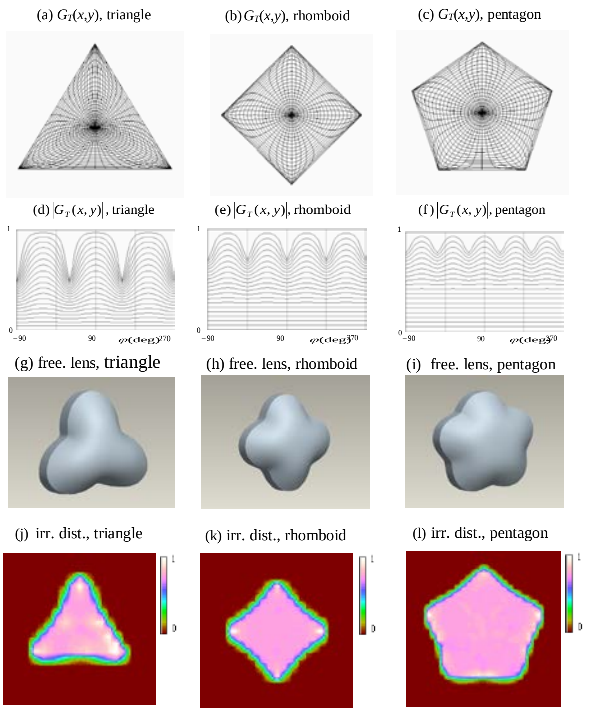

Fig. 6 Proposed source-target maps, freeform lens and irradiance distribution for three right polygons.

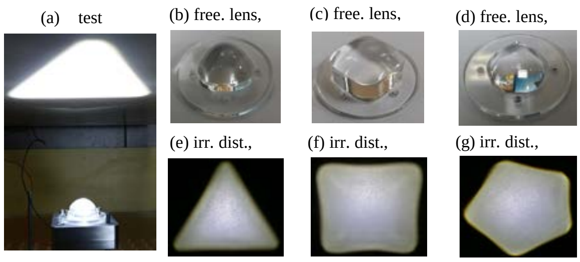

Fig. 7 Experimental test setup, freeform lenses for uniform polygonal illumination, and experimental results.

CONCLUSIONS

Very few of previous studies have taken into account the smoothness of the source-target map in design of a freeform lens. It may result in a lens with discontinuous surfaces or surfaces with bulge/sharp edges that will greatly increase the difficulty for the lens fabrication and induce large variation in the produced irradiance distribution. Hence, a smooth source-target map for uniform polygonal illumination is proposed to solve the problem.

In the proposed map, the polygon is divided into a number of symmetric quadrilaterals of the same size. Meanwhile, the irradiance energy of source is divided into the same number of symmetric pie sectors. The proposed map is an integration of a number of primitive maps after scaling and rotation.

The proposed primitive map is described by Eqs (8) and (9) using the area-affine coordinate system of Eqs (7). Procedures to implement the proposed map are given in this study. Freeform lenses designed for uniform polygonal illumination have been manufactured in PMMA by CNC machining. Despite that the freeform surfaces have 0.03mm imprecision due to labor-intensive polishing, precise illumination profiles and good uniformity of irradiance distribution are achieved.

The contribution of this study is fundamental and profound in the field of freeform lens design. Advanced studies for uniform illumination of arbitrary polygons are currently taken to expand the applicability of the proposed map.

ACKNOWLEDGMENTS

This work was supported by the Ministry of Science and Technology, R.O.C., under the grant NSC 106-2221-E-168-010-. Thanks for the suggestions of the anonymous reviewers to help enhance the quality of this paper.

REFERENCES

Chen, F., Wang, K., Qin, Z., Wu, D., Luo, X., and Liu, S., “Design method of high–efficient LED headlamp lens,” Opt. Express, Vol. 18, No. 20, pp. 20926–20938 (2010).

Ding, Y., Liu, X., Zheng, Z., and Gu, P., “Freeform LED lens for uniform illumination,” Opt. Express, Vol. 16, No. 17, pp. 12958–12966 (2008).

Fang, F., Zhang, X., and Hu, X., “Cylindrical coordinate machining of optical freeform surfaces,” Opt. Express, Vol. 16, No. 10, pp. 7323-7329 (2008).

Fournier, F., Cassarly W., and Rolland, J., “Fast freeform reflector generation using source-target maps,” Opt. Express, Vol. 18, No. 5, pp. 5295-5304 (2010).

Lin, K.C. “Smooth energy mappings for freeform lens design,” Opt. Rev. , Vol. 21, No. 5, pp. 639-641 (2014).

Luo, Y., Feng, Z., Han, Y., and Li, H., “Design of compact and smooth freeform optical system with uniform illuminance for LED source,” Opt. Express, Vol. 18, No. 9, pp. 9055–9063 (2010).

Mao, X., Li, H., Han, Y., and Luo, Y., “Polar-grids based source-target mapping construction method for designing freeform illumination system for a lighting target with arbitrary shape,” Opt. Express, Vol. 23, No. 4, pp. 4313-4328 (2015).

Ries, H. and Rabl, A., “Edge-ray principle of nonimaging optics,” J. Opt. Soc. Am. A, Vol. 11, No. 10, pp. 2627–2632 (1994).

Ries, H. and Muschaweck, J., “Tailored freeform optical surfaces,” J. Opt. Soc. Am. A, Vol. 19, No. 3, pp. 590–595 (2002).

Wang, K., Liu, S., Chen, F., Liu, Z., and Luo, X., "Effect on manufacturing defects on optical performance of discontinuous freeform lens," Opt. Express, Vol. 17, No. 7, pp. 5457–5465 (2009).
Wu, R., Benítez, P., Zhang, Y., and Miñano, J., "Influence of the characteristics of a light source and target on the Monge–Ampére equation method in freeform optics design," Opt Lett, Vol. 39, No. 3, pp. 634-637 (2014).
Xia, L., Yin, S., Dong, X., and Du, C., "Multi-segment freeform LED uniform lens with low reflective loss," Proc. of SPIE 7849, 784910–1-6 (2010).

正多邊形均光照明自由曲面透鏡之平滑光能量映射設計

林穀欽　　馬敏雄
崑山科技大學機械工程學系

摘 要

本文提出一連續且平滑自由曲面透鏡設計法，本透鏡可將一朗伯分佈光能量映射至一目標平面，使其呈現正多邊形之均光照明區域。本設計法將所有光源輸出能量分割成多個大小相同且對稱之扇形光能量，並將正多邊形照明區域分割成多個大小相同且對稱之四邊形照明區域，因此本映射可由多個基元映射所合成，其中每一基元映射乃將扇形光能量映射至四邊形照明區域。本文提出基元映射設計之步驟，並以蒙地卡羅光跡模擬以及實作，以驗証本設計法之正確性。